Paper presented at the "16th European Photovoltaic Solar Energy Conference and Exhibition,"
Scottish Exhibition + Conference Centre Glasgow, United Kingdom 1 - 5 May 2000

INVESTIGATIONS ON MICROSTRUCTURE AND MICROCHEMISTRY OF POLYCRYSTALLINE SILICON MATERIALS FOR SOLAR CELLS

M. Stöger[1], P. Schattschneider[1], W. Markowitsch[2], V. Schlosser[2], R. Schneider[3], H. Kirmse[3], W. Neumann[3]
[1]Institute of Applied and Technical Physics, Vienna University of Technology, Austria
[2]Institute for Material Physics, University of Vienna, Austria
[3]Humboldt University of Berlin, Institute of Physics, Chair of Crystallography, Germany

ABSTRACT: A p-i-n doped μc-silicon thin film grown by means of hot wire chemical vapour deposition (HW CVD) on a zinc oxide film was investigated by transmission electron microscopy (TEM) and electron energy loss spectroscopy (EELS). The structure of both layers, the ZnO substrate layer as well as the silicon thin film, and the chemical composition at the interface were the subjects of our investigations. We observed that a layer of pure (nearly oxygen-free) silicon with a thickness of about 5 nm covered the substrate surface. A reliable model to derive information about the texture of the interface between ZnO and μc-Si, the origin and the thickness of the oxygen-poor Si-layer was developed.
Keywords: Micro Crystalline Silicon – 1: ZnO – 2: Thin Film – 3

1. INTRODUCTION

Thin films of crystalline silicon offer considerable potential for a stable and low cost solar cell technology [1, 2]. With light trapping, even films with thicknesses of only ≈ 10 µm can absorb about 90 % of the incoming sun light. To fully realize this potential, it will be essential not only to develop appropriate cell structures which provide the neccessary optical confinement, but also to do so on low cost substrates such as glass. Glass is, in principle, the ideal substrate as far as costs and the manufacturing of large areas are concerned. However, its incapability of resisting processing temperatures larger than about 550 °C places severe restrictions on crystalline silicon deposition and solar cell manufacture.

In the recent years, micro-crystalline silicon thin films have attracted much attention for photovoltaic applications [3]. Their advantage is the combination of low temperature deposition techniques, similar to amorphous silicon, and a very low cell degradation during operation, similar to crystalline silicon solar cells. To achieve high deposition rates and stimulating crystallite formation, the deposition technique is usually accompanied by providing an additional energy source in the deposition system. In this paper we report about investigations of μc-Si thin films produced by hot wire CVD (HW CVD) – sometimes also referred to as catalytic CVD [4] – on ZnO substrates. This process allows fairly high deposition rates as well as good control of the doping process. In particular, we report on the diffusion of ZnO from the electrical contact layer into the silicon thin film and on a silicon-enriched interlayer with reduced oxygen content at the ZnO-Si interface.

2. EXPERIMENTAL TECHNIQUES

The studied micro-crystalline silicon thin film was deposited on a polycrystalline ZnO layer in a HW CVD multichamber reactor equipped with a load-lock chamber and base pressures lower than 10^{-8} mbar. The polycrystalline ZnO layer itself was deposited on a CORNING 7059 wafer glass under low temperature conditions (about 200 °C) and served as a transparent conductive oxide (TCO) layer.

The thicknesses and the substrate temperatures of the deposited layers in this multilayer system are given in Table I. A gas flow consisting of 1 sccm and 19 sccm of silane and hydrogen, respectively, was used in the deposition chamber. The dissociation was obtained by means of a hot tungsten wire with a diameter of 1.0 mm at a temperature of about 1740 °C. The process pressure was $7x10^{-3}$ mbar. The ZnO/glass substrate was held at about 200 °C during the film growth. Doping of the silicon film was performed by adding di-Boran or Phosphine, respectively, to the gas mixture. From the grown films, the specimens for the present study were prepared by mechanical thinning and ion milling. Two pieces of the samples were glued together face-to-face with M-Bond 600 glue in order to obtain a cross sectional preparation. After ion milling the sample was immediately transferred into the TEM to minimize the oxidation, which would be caused by long-term exposure to ambient air. The films were investigated by transmission electron microscopy (TEM), electron energy loss spectrometry (EELS) and by energy filtered TEM (EFTEM), which enabled us to create one- and two-dimensional maps of the concentration of each element of interest. The three-window technique was applied for EFTEM, i.e. measurements in the pre- and post-edge region were done for calculating the signal background with a power-law fit. In order to obtain the pure elemental signal, this correction was necessary, because the background depends on the thickness and on the matrix of the specimen. The correction corresponding to the different mean free paths of the ZnO and *pc*-Si layers followed the procedure proposed by Hofer et al. [5].

Table I: Composition of the multilayer thin film system

	dopant	thickness [µm]	temperature [°C]
ZnO	-	0.33	-
p-Si	B	≈ 0.1	175
intrinsic Si	-	≈ 0.8	215
n-Si	P	≈ 0.05	215

All measurements were carried out on a Hitachi H-8110 200-kV TEM microscope accompanied with a GATAN imaging filter (GIF) system and a scanning unit. In the STEM mode series of EEL spectra were taken by means of the GATAN digiscan.

3. RESULTS AND DISCUSSION

In previous investigations [6] we have observed, that some of the ingredients of the substrate tend to penetrate the thin Si film even at deposition temperatures of only ≈ 200 °C. Therefore the behaviour of ZnO at the interface was of particular interest in the present study. Three different methods of EELS-analysis were performed:

- EELS measurements in the image mode of the TEM with high spatial resolution;
- EELS measurements in the STEM mode;
- energy filtered TEM (EFTEM): generating an elemental map by means of an energy filter.

All measurements were taken at different positions on the specimen to exclude untypical local effects and to improve statistics.

The advantage of the first method is the high spatial resolution, which depends only the magnification of the microscope and the width of the GIF entrance slit. Table II gives the total counts for Zn in the post-edge region in an interval of 130 eV after background correction. The listed values demonstate that Zn is mixed with Si during the deposition.

Table II: Total number of counts for the Zn-$L_{2,3}$ edge after background substraction.

distance from the ZnO/Si interface [nm]	number of counts
-10	677 679
0	226 364
5	102 966
12	96 267
17	21 368
22	0

Figure 1 shows three-dimensional maps of the Zn and Si distributions in the vicinity of the interface obtained by EFTEM. The distance between subsequent line profiles is 5 nm.

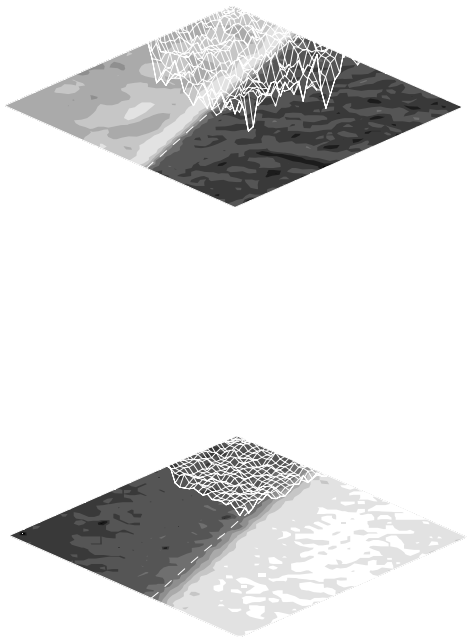

Figure 1: 3-d plots of the Si concentration (upper panel) and the Zn concentration (lower panel) at the Si-ZnO interface. Note that the concentration is plotted inversely.

From Fig. 1 it can be clearly recognized that very close to the interface a layer of enhanced Si concentration is formed. The thickness *d* of this layer is 5.4 ± 1.6 nm. Our investigations showed, that the thickness of this Si "rampart" depends on the local texture of the interface. Additionally, Fig. 1 as well as Table II demonstrate that ZnO is also present on the Si side of the interface, and that Si is detected in the ZnO region, too. The latter may be understood by the reaction of ZnO with the atomic hydrogen during the initial stage of the depostition process. Hydrogen reduces ZnO to elemental Zn. Thereby, pores are built at the ZnO surface and, later, Si fills these pores.

In Fig. 2 a bright-field TEM image shows the structure of the ZnO-Si interface in more detail. We observe in the figure that the ZnO surface has a wavy texture. The dark regions in the lower part of Fig. 2 are the ZnO crystallites, and the bright band is the pure Si layer. The average width *w* of this wavy region is about 8 nm. The width of the interface region can therefore be defined as $w + d$ and has an extension of 13.1 ± 1.6 nm.

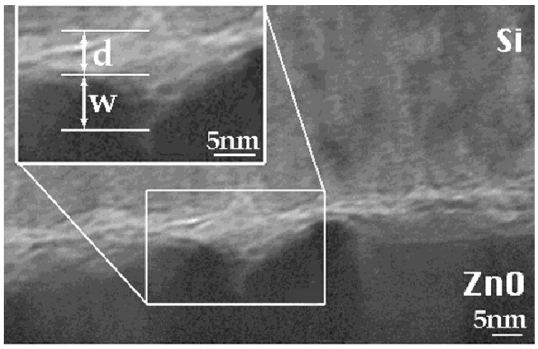

Figure 2: Bright-field TEM image of the Si-ZnO interface. The inset demonstrates the thickness *d* of the Si-enriched layer and the surface roughness *w* of the ZnO substrate.

Since no elements other than Si, Zn, and O were detected inside the *μc*-Si layer, the oxygen distribution can be regarded as a proof of the purity of silicon at the interface with respect to ZnO contamination. Fig. 3 shows line profiles across the interface, measured with the GIF system and averaged over a region of 150 x 120 nm^2. The upper panel in Fig. 3 displays the total oxygen contents. Assuming that zinc is present only as stoichiometric ZnO, the Zn distribution is set equal to the oxygen distribution of ZnO. By subtracting the "ZnO-oxygen" distribution (middle panel in Fig. 3) from the former we get a excess oxygen distribution in the Si-layer (lower panel in Fig. 3), which is the concentration of oxygen that is not bound to Zn. The results in Fig. 3 demonstate that nearly all the oxygen on the ZnO side of the interface is incorporated in ZnO, whereas on the Si side additional oxygen is present.

Moreover, it can be clearly recognized from Fig. 3 that the Si close to the interface is less contaminated by oxygen. A plausible reason is that the oxygen that contaminates the sample during the preparation reacts primarily with the metallic zinc, which was reduced by the atomic hydrogen that is a product of the dissociation of SiH_4 in the HW CVD reactor. As a consequence, silicon is deposited in a very pure form onto the rough ZnO layer surface. When the entire surface is covered by the oxygen-poor Si layer the oxygen is integrated into the silicon, thus leading to a lower Si concentration.

A further topic of our investigation was the oxygen distribution not only close to the interface, but throughout the entire Si layer. To address this item, we took energy-loss linescans with measurements at every 130 nm. The results are shown in Table III. Close to the sample surface (i.e. far from the interface), the oxygen concentration is

slightly enhanced due to the oxidation by the ambient air. However, since the layer is porous, oxygen is able to diffuse into the inner regions. Near the interface the oxygen concentration is slightly reduced, because the layer is boron doped. It is well-known that boron doping supports a compact and almost defect-free crystal growth, which hampers the oxygen diffusion.

Table III: Oxygen concentration as a function of the distance from the ZnO-Si interface.

distance [nm]	oxygen concentration [%]
130	17
260	25
390	19
520	17
650	22
780	21
910	22
1040	25
1170	28

The compactness of the Si in the B-doped region is well illustrated by Fig. 4, which presents a dark-field image of the *μc*-Si layer near the interface. The first 100 nm measured from the interface are obviously illuminated more brightly. This indicates a higher density of crystals oriented in the same crystallographic direction.

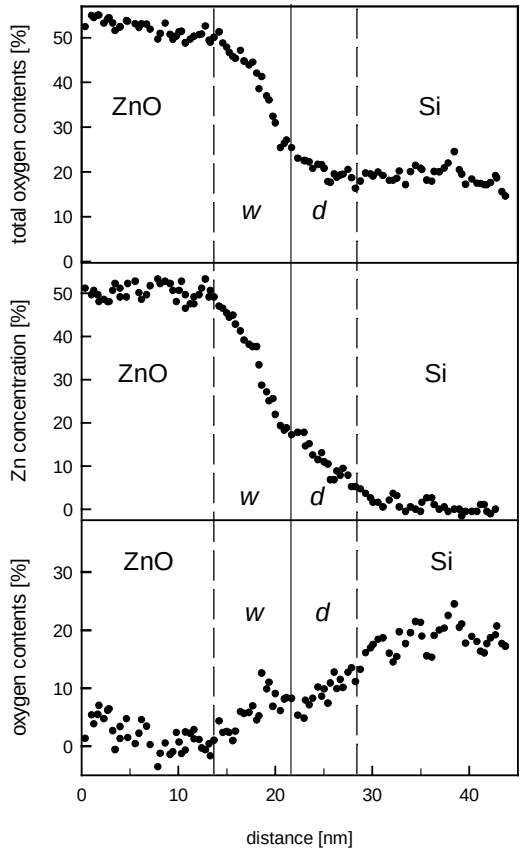

Figure 3: Line profiles of the concentrations of oxygen and Zn near the ZnO-Si interface. Upper panel: total oxygen contents. Middle panel: the contents of oxygen bound to Zn. The lower panel displays the difference of the upper two curves, and shows the concentration of excess oxygen that is not incorporated in ZnO.

A bright-field image of he interface region is shown in Fig. 5. Obviously, the growth of crystallites starts directly at the interface. The dark regions within the *μc*-Si part represent the compact regions induced by boron doping.

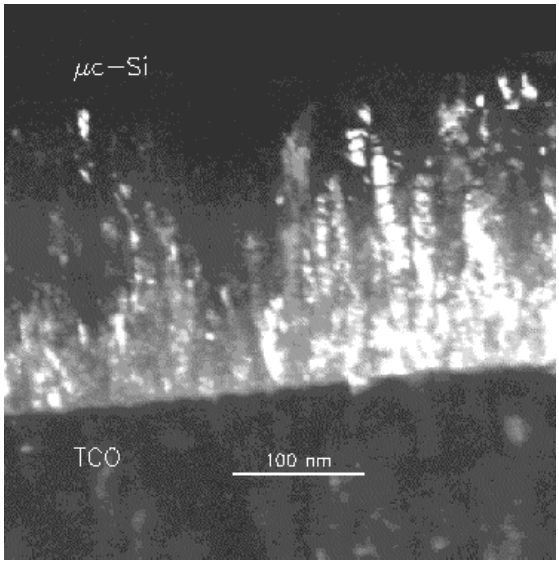

Figure 4: Dark-field image of the *μc* Si film. Close to interface a significantly larger number of microcrystals is illuminated, indicating an enhanced density of crystals aligned in the same direction.

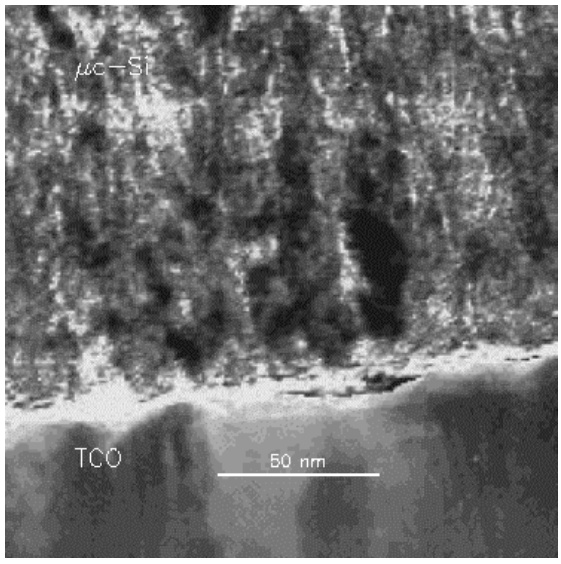

Figure 5: Bright-field image of the ZnO-Si interface. Apparently, the growth of Si crystallites starts right from the interface.

4. CONCLUSIONS

Our investigations show that a mixture of Si and ZnO is present at the interface between the ZnO layer, which is used as a transparent electrical contact material, and the *μc*-Si thin film, which acts as the light absorber. It seems to be likely, that the presence of atomic hydrogen at the beginning of the deposition process reduces the surface

of the ZnO layer to metallic Zn. As shown in Fig. 2, the interface becomes rough, and little pores are enlarged at the grain boundaries. Afterwards, oxygen preferently reacts with the elemental Zn, thereby re-forming and depositing ZnO. Hence we assume that, within the first few nanometers, the Si is deposited nearly oxygen-free until the entire surface of the ZnO substrate is covered. However, oxidized Zn is still present in that layer. The roughness w of the interface and the thickness d of the oxygen-free Si layer can be estimated from the concentration profiles in Fig. 3. The interface region, given by $w + d$ is about 13 nm thick. However, a certain degree of diffusion of both zinc and silicon into the other layer cannot be completely ruled out.

The unindentionally introduced texture of the interface is too smooth for effective light trapping as needed in thin film solar cells. The width of the interface region of about 13 nm must be compared with the average diameter of the needle-like ZnO crystals, which is about 20-40 nm according to Figs. 2 and 5. Thus, the ratio of height to width of the texture is only ≈ 0.3; a value of ≈ 1 would be more appropriate. In order to improve the above ratio and thus improving the light trapping structure of the interface, ZnO crystals with smaller diameters should be used.

5. ACKNOWLEDGEMENTS

This work has been supported by the JOULE project "CRYSTAL", contract nr. JOR-CT47-0126 of the European Commission. The authors would like to thank Prof. Dr. J. Andreu from the Department of Physics and Electronics of the University of Barcelona for providing the samples.

REFERENCES

[1] J. H. Werner, R. Bergmann, R. Brendel, Advances in Solid State Tech. **34** (1994) 153
[2] Z. Shi, S. R. Wenham, Prog. in Photovoltaics **3** (1994) 153
[3] S. K. Deb, Curr. Opin. Solid State Mat. Sci **3** (1998) 51
[4] R. Iiduka, A. R. Heya, H. Matsumura, Sol. Energy Mater. Sol. Cells **48** (1997) 279
[5] F. Hofer, W. Grogger, G. Kothleitner, P. Warbichler, Ultramicroscopy **67** (1996) 83
[6] M. Stöger, M. Nelhiebel, P. Schattschneider, V. Schlosser, A. Breymesser, B. Jouffrey, submitted to Sol. Energy Mater. Sol. Cells